HNUE JOURNAL OF SCIENCE
Natural Sciences 2024, Volume 69, Issue 2, pp. 78-89
This paper is available online at http://hnuejs.edu.vn/ns
DOI: 10.18173/2354-1059.2024-0022

STUDY ON THE CO_2 ADSORPTION PROPERTIES OF ACTIVATED CARBON PRODUCED FROM CORN COB

Luong Thi Thu Thuy and Le Van Khu*
Faculty of Chemistry, Hanoi National University of Education, Hanoi city, Vietnam
*Corresponding author: Le Van Khu, email: khulv@hnue.edu.vn

Received March 7, 2024. Revised June 19, 2024. Accepted June 26, 2024.

Abstract. Activated carbon (AC) prepared from corn cobs was used as an adsorbent for CO_2 capture under different temperatures. The characterization by Boehm titration and TGA showed that the total acidic groups of AC were significantly higher than the total basic groups, and the increasing activated temperature resulted in increases in the total basicity and decreases in the total acidity. The CO_2 adsorption behavior of AC was predicted by four isotherm models. It was found that the suitable order was Sips > Tóth > Freudlich > Langmuir. The maximum monolayer coverage capacity and isosteric heat of adsorption were in the range of 6.28 - 10.92 mmol g^{-1} and 26.48 - 21.55 kJ mol^{-1}, respectively. High specific surface area and high amount of carboxylic groups were found to be in favor of CO_2 capture.

Keywords: adsorption, CO_2, activated carbon, isotherm, isosteric heat.

1. Introduction

Over the past few decades, rapid industrialization has led to a tremendous increase in the amount of CO_2 released into the atmosphere, which has inevitably resulted in an increased risk of global warming [1]. Human activities are influencing the carbon cycle by adding more CO_2 to the atmosphere as well as influencing the ability of natural sinks to remove CO_2. The main anthropogenic CO_2 sources include those from power generation, transportation, industrial and agricultural sources. CO_2 has become a leading concern of nations worldwide. Many countries are actively engaged in research in this area and have released vehicle and power plant emissions standards [2]. To comply with those limits, industries need to reduce CO_2 residual in their emissions to acceptable levels. The methods commonly employed for the removal of CO_2 utilize carbon capture and storage technologies, namely adsorption, absorption, and membrane separation technology [3]. The main drawback of current commercial CO_2 capture technologies is their high costs and energy consumption. In this aspect, in comparison with other methods, adsorption appears to be a reasonable alternative. A variety of porous materials

including zeolites [4], porous carbon [5], mesoporous silica [6], and metal-organic frameworks [7] have been reported on extensively. Due to their low cost, high availability, hydrophobicity, large surface area, controllable pore structure, and chemical stability, activated carbon is a promising material for CO_2 adsorption.

Activated carbon can be prepared from some agricultural waste such as rice husks, straws, and corn cobs. Corn is grown widely in many regions and is one of the major agricultural products of Vietnam, with about 4 million tons produced annually. Currently, only a small portion of corn cobs has been used for incineration and mushroom cultivation, the remaining portion is just burned on the fields causing environmental pollution. Like other grain fibers, corn cob consists predominantly of cellulose and hemicellulose [8], which are high in carbon content and are ideal for the manufacture of activated carbon.

In our previous work [9], AC was successfully synthesized from corn cobs with KOH as an activating agent and has been used as supercapacitor electrode material, showing that corn cob base activated carbon has good electrochemical properties. To expand research in application for the gas adsorption and separation fields, this article will study and discuss the CO_2 adsorption properties of AC from corn cobs.

2. Content

2.1. Experiments

2.1.1. Preparation of activated carbon

Activated carbon from corn cobs was prepared by chemical activation with KOH as a chemical activating agent as pointed out in our previous work [9]. In brief, the prepared corn cobs were first carbonized at 450 ^oC for 90 min in a nitrogen atmosphere, then the carbonized products were impregnated with KOH (weight ratios char: KOH ratio of 1 : 3). The activation process was performed under a nitrogen flow of 300 mL min^{-1} and at a preset temperature in the range of 700 - 850 ^oC in 90 min. The prepared carbon was neutralized by 0.1 M HCl solution, washed with hot distilled water, and then dried and stored in a desiccator ready for use. The samples were labeled as AC-700, AC-750, AC-800, and AC-850 according to activation temperatures.

2.1.2. Characterization of activated carbons

Textural properties of the AC samples were measured from N_2 adsorption/desorption isotherms at 77 K (Micromeritics, TriStar 3020). The obtained results were presented in our previous work [9] and shown in Table 1 for ease of follow-up.

Table 1. Physical properties deduced from N_2 adsorption at 77 K on AC samples

Sample	S_{BET} (m^2g^{-1})	S_{mic} (m^2g^{-1})	S_{ext} (m^2g^{-1})	V_{mic} (cm^3g^{-1})	V_{ext} (cm^3g^{-1})	V_{tot} (cm^3g^{-1})	S_{mic}/S_{BET} (%)	V_{mic}/V_{tot} (%)
AC-700	1496	1468	28	0.6470	0.0413	0.6883	98.1	*94.0*
AC-750	1752	1718	34	0.7696	0.0518	0.8214	98.1	*93.7*
AC-800	1740	1719	21	0.7374	0.0320	0.7694	98.8	*95.8*
AC-850	*2331*	*2283*	*48*	*1.0413*	*0.0696*	*1.1109*	*97.9*	*93.7*

The surface acidity and basicity of AC samples were determined by Boehm titrations [10]. The numbers of acidic sites were calculated under the assumption that NaOH reacted with all groups (carboxyl, phenolic, and lactonic); Na_2CO_3 did not react with phenolic groups; and $NaHCO_3$ only reacted with carboxyl groups. The numbers of basic sites were calculated from the amount of hydrochloric acid consumed by the AC samples.

Thermogravimetric analysis was performed using a Shimadzu thermal analyzer model DTG-60H in argon atmosphere at a heating rate of 10 $^oC\ min^{-1}$.

2.1.3. Adsorption test

The adsorption of CO_2 was performed on a Micromeritics TriStar 3000 analyzer. Before each measurement, the activated carbon sample was degassed in the N_2 atmosphere at 150 ^oC for 8 h. A precise amount of AC sample (about 300 mg) was placed in a measuring tube, evacuated to remove all gases, and immersed in a water bath at preset temperatures (5, 15, 25, and 35 ^oC) for 60 min to ensure the sample temperature was balanced with the heating bath. The measurement was then performed automatically in an equilibrium pressure of CO_2 in the range of 1 - 132 kPa.

2.2. Results and discussion

2.2.1. Characterization of the as-prepared activated carbon samples

The results of Boehm titration are depicted in Table 2. It could be observed that the total acidity was significantly higher than the total basicity, 1.512 - 2.852 mmol/g acidic groups and only 0.214 - 0.349 mmol/g basic groups. The increasing activated temperature resulted in the decrease of acidic groups and the increase of basic groups. Acidic groups decomposed at the range of 150 - 650 ^oC, meanwhile, basic groups decomposed at the range of 650 - 980 ^oC [11], hence, the acidity decreased at higher activation temperature. However, as surface oxygen groups were removed from the activated carbon, the delocalized π-electrons of the basal planes were strengthened, which contributes to the basic property of activated carbon, therefore, the basicity of activated carbon increased slightly at high temperature.

Table 2. Results of Boehm titration

Sample	Groups			Total acidity (mmol g^{-1})	Total basicity (mmol g^{-1})
	Carboxyl (mmol g^{-1})	*Lactonic (mmol g^{-1})*	*Phenolic (mmol g^{-1})*		
AC-700	1.365	0.906	0.581	2.852	0.214
AC-750	0.557	0.482	0.648	1.687	0.300
AC-800	0.769	0.916	0.298	1.983	0.331
AC-850	0.450	0.812	0.250	1.512	0.349

The TGA diagram of the AC samples measured in the argon atmosphere is shown in Figure 1. Three main steps could be differentiated: (i) below 200 ^oC, the weight loss of AC samples was not so obvious, below 1.365% for all AC samples, this was due to the loss of moisture or crystalline water and the decomposition of carboxyl group; (ii)

between 200 and 400 ^oC, the weight loss of AC samples was higher, the AC-700 lost 4.128% of its weight and AC-850 lost 2.570%, this weight loss corresponds to the degradation of the remaining carboxyl and lactonic groups [11]; (iii) after 400 ^oC, there was a significant weight loss due to the combustion of activated carbon. The weight loss of all AC samples in two temperature ranges 100 - 200 ^oC and 200 - 400 ^oC was consistent with the amount of carboxyl and carboxyl + lactonic obtained from Boehm titration (Figure 2a, b). These results complemented and confirmed the results of Boehm titration.

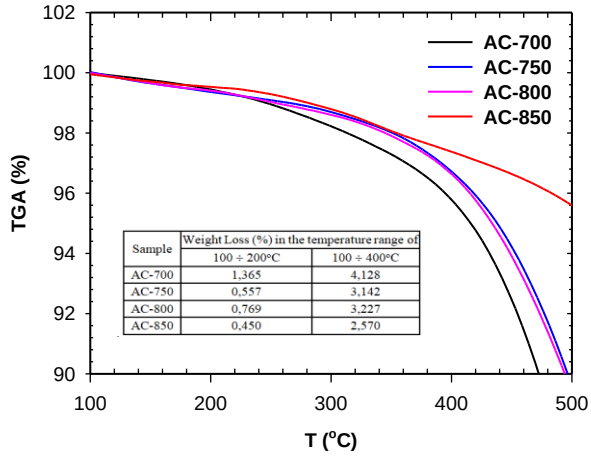

Figure 1. TGA diagram of the AC samples

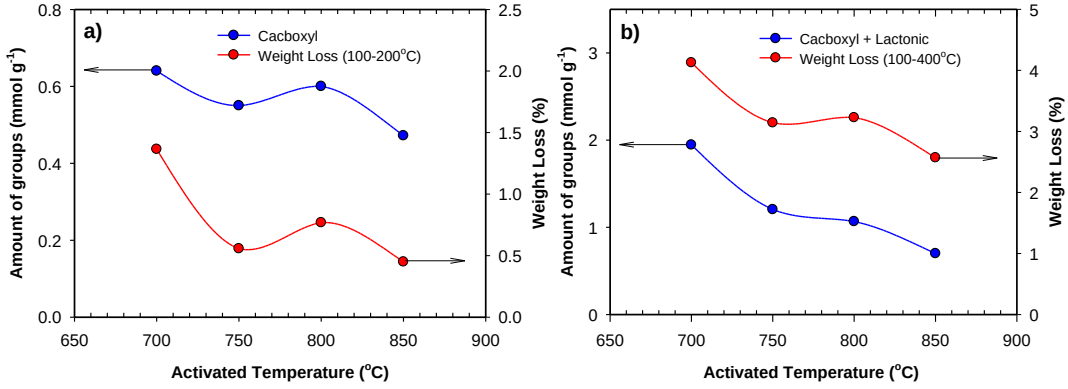

Figure 2. Correlation between TGA and Boehm titration of (a) carboxyl group and (b) carboxyl+lactonic groups

2.2.2. CO_2 adsorption isotherm

The adsorption isotherm of CO_2 on AC samples at 25 ^oC is shown in Figure 3. According to this figure, CO_2-adsorbed amounts increased with increasing CO_2 pressure. Within the studied pressure range, the CO_2 adsorption capacity of the samples gradually increased in the order AC-700 < AC-750 ≈ AC-850 < AC-800. The smallest adsorption capacity value of AC-700 was due to its smallest specific surface area and micropore volume [12] (1496 $m^2\ g^{-1}$ and 0.6470 $cm^3\ g^{-1}$).

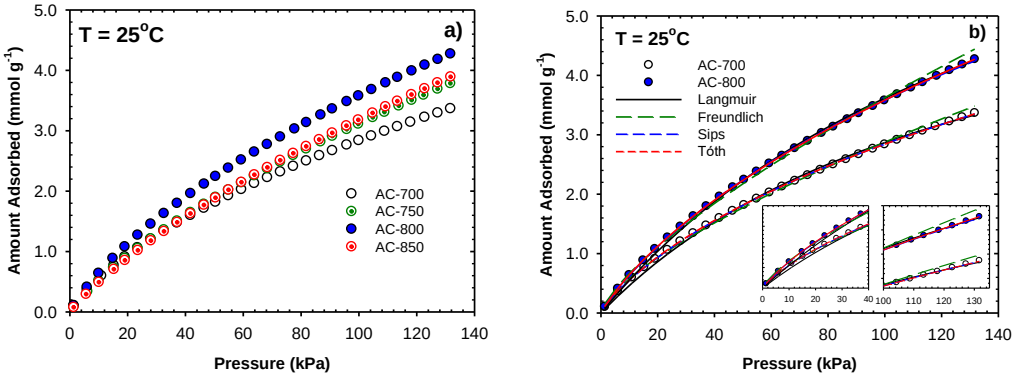

Figure 3. a) Adsorption isotherms of CO_2 on AC samples at 25 °C, b) Modeling of adsorption isotherms of CO_2 on AC-700 and AC-800 at 25 °C

Although the specific surface area and micropore volume of the AC-800 sample (1740 m^2 g^{-1} and 0.7374 cm^3 g^{-1}) were similar to the AC-750 sample (1752 m^2 g^{-1} and 0.7696 cm^3 g^{-1}) and lower than that of AC-850 sample (2331 m^2 g^{-1} and 1.0413 cm^3 g^{-1}), it had a much larger CO_2 adsorption capacity. This was due to the larger amount of carboxyl functional group in the AC-800 sample since carboxyl groups added a negative charge to the surface, improved the surface polarity, provided Lewis bases reaction, and enhanced bonding reaction with CO_2 [13].

**** Modeling of adsorption isotherms***

The experimental data were analyzed using four popular isotherm models including Langmuir, Freundlich, Sips, and Toth [14]. The expressions of these isotherms are listed in Table 3.

Table 3. Adsorption isotherm models

Isotherm model	Isotherm model expression	Parameters	Constraint
Langmuir	$q_e = q_m \frac{K_L.P}{1+K_L.P}$	q_m: maximum monolayer coverage capacity K_L: Langmuir isotherm constant	-
Freundlich	$q_e = K_F.P^{\frac{1}{n}}$	K_F: Freundlich isotherm constant n: parameter related to multiple layer coverage	n > 1
Sips	$q_e = q_{m_S}.\frac{(bP)^{n_S}}{1+(bP)^{n_S}}$	q_{mS}: Sips maximum adsorption capacity b: Sips equilibrium constant n_S: Sips model exponent	0 < n < 1
Tóth	$q_e = \frac{q_e^{\infty}P}{\left[K_{Th}+P^{Th}\right]^{\frac{1}{Th}}}$	q_e^{∞}: Tóth maximum adsorption capacity K_{Th}: Tóth equilibrium constant Th: Tóth model exponent	$0 < \frac{1}{Th} < 1$

The hybrid fractional error function (HYBRID) was used to evaluate the parameters of these four isotherm equations. The coefficient of determination (R^2) and the average relative errors (ARE) were used to determine the correlation between experimental data and the isotherm equation and the fit between the experimental and predicted values for adsorption capacity.

$$HYBRID = \frac{100}{N-p}\sum_{i=1}^{N}\left[\frac{\left(q_{e,pre}-q_{e,mes}\right)^2}{q_{e,mes}}\right]_i \quad (1)$$

$$R^2 = 1-\frac{\sum_{i=1}^{N}(q_{e,mes}-q_{e,pre})_i^2}{\sum_{i=1}^{N}(q_{e,mes}-q_{e,mean})_i^2} \quad (2)$$

$$ARE = \frac{100}{N}\sum_{i=1}^{N}\left|\left(\frac{q_{e,pre}-q_{e,mes}}{q_{e,mes}}\right)_i\right| \quad (3)$$

where $q_{e,mes}$ and $q_{e,pre}$ are the experimental and predicted adsorption capacities, respectively; N is the number of experimental data; p is the parameter of the isotherm equation.

The R^2 and ARE values obtained from the fitting of experimental data by four isotherm models were summarized in Table 3. The isotherms of the two samples, AC-700 and AC-800, fitted by Langmuir, Freundlich, Sips, and Tóth models were introduced in Figure 3.

Table 4. The R^2 and ARE values correspond to the different isothermal models

Sample	Isotherm	R^2	ARE(%)
AC-700	Langmuir	0.9976	4.42
	Freundlich	0.9974	3.26
	Sips	**0.9999**	**0.75**
	Tóth	0.9999	0.82
AC-750	Langmuir	0.9982	2.94
	Freundlich	0.9982	2.92
	Sips	**0.9998**	**0.70**
	Tóth	0.9999	0.72
AC-800	Langmuir	0.9986	3.68
	Freundlich	0.9969	3.52
	Sips	**0.9999**	**0.63**
	Tóth	0.9999	0.65
AC-850	Langmuir	0.9947	2.70
	Freundlich	0.9982	2.72
	Sips	**0.9999**	**0.52**
	Tóth	0.9999	0.59

From Table 3, it was notable that all four models had an R^2 value which was close to 1, showing strong matches between the experimental data and the chosen models. This correlation was also observable in Figure 3 in which the fitting lines passed by most of the experimental points, except for the Freundlich model at elevated pressure and the Langmuir at low pressure. However, the ARE values when applying the Langmuir and Freundlich equations were rather high, being in the range of 2.70 - 4.42% and 2.72 - 3.52%, respectively. Meanwhile, the ARE values of the Sips and Tóth models were both less than 1%. In particular, the ARE value of the Sips model (0.52 - 0.75%) was always the lowest of all the models studied. The suitable order of these four models, according to R^2 and ARE, was Sips > Tóth > Freundich > Langmuir. However, the Langmuir model allows for easily calculating the maximum monolayer coverage capacity, which is often used to compare the adsorption capacity of samples. Therefore, the best-fitted model, Sips, and the most convenient model for comparison, Langmuir, will be further investigated in the following section.

**** Influence of adsorption temperature***

Figure 4 introduced the CO_2 adsorption isotherms of AC samples at adsorption temperatures ranging from 5 to 35 ^oC. The capacity of CO_2 adsorption of all samples decreased slightly with an increasing adsorption temperature, indicating the exothermic nature of the adsorption process [15]. The decline of the adsorption capacity was due to the lessening of binding forces between CO_2 and activated carbon at elevated adsorption temperatures.

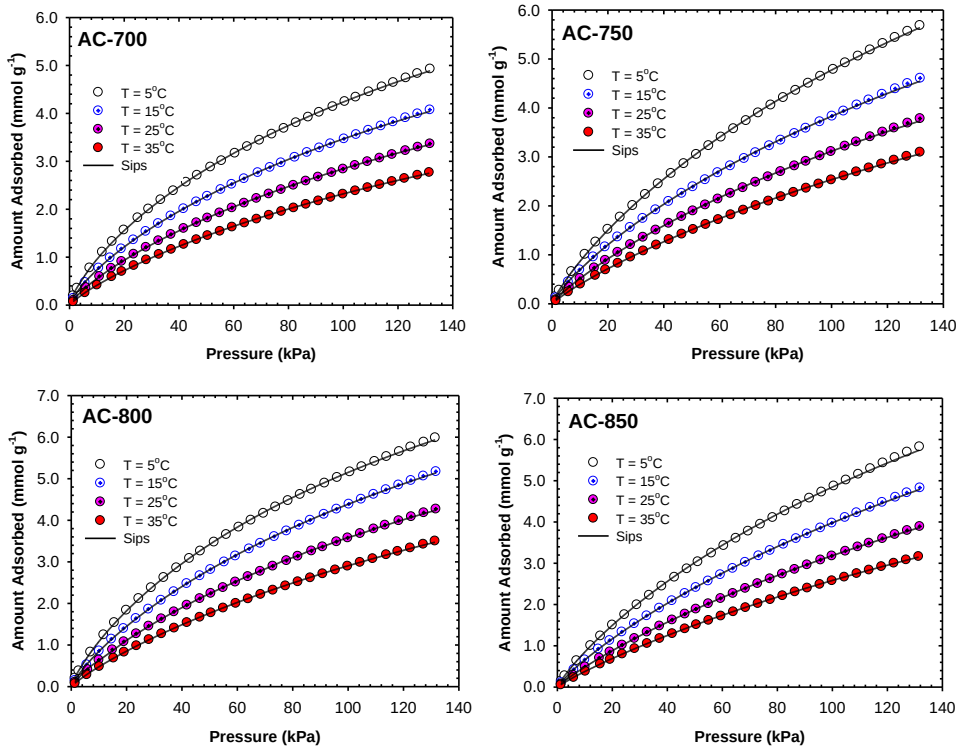

Figure 4. The CO_2 adsorption isotherms of AC samples at different adsorption temperatures

The experimental data were fitted with the Langmuir and Sips models and the obtained data were summarized in Table 5. The maximum monolayer coverage capacity of AC-700, AC-750, AC-800, and AC-850 samples at 5, 15, 25, and 35 ^oC was in the range of 8.36 - 6.28 mmol g^{-1}, 9.81 - 7.15 mmol g^{-1}, 10.92 - 8.35 mmol g^{-1}, and 10.42 - 7.25 mmol g^{-1}, respectively. These values are considerably high compared to other literature [16], proving that AC from corn cob was capable of adsorbing CO_2 under normal conditions. The high adsorption capacity of AC-800 could be explained by the simultaneous influence of specific surface and carboxyl functional groups as mentioned above. Besides, q_m and K_L were decreased with increasing temperature, affirming the exothermic adsorption process.

Table 5. Parameters of the Langmuir and Sips isotherms for the adsorption of CO_2 onto activated carbon at different temperatures

Sample	Isotherm	Parameters	5 ^oC	15 ^oC	25 ^oC	35 ^oC
AC-700	Langmuir	q_m (mmol g^{-1})	8.36	7.53	6.84	6.28
		K_L	0.0105	0.0087	0.0072	0.0059
		R^2	0.9963	0.9968	0.9976	0.9983
		ARE(%)	**5.75**	**4.88**	**4.42**	**3.99**
	Sips	q_{mS} (mmol g^{-1})	13.77	13.04	11.45	9.30
		$b(kPa)^{-n_S}$	0.0035	0.0027	0.0026	0.0028
		n_S	0.777	0.783	0.815	0.855
		R^2	0.9999	0.9999	0.9999	0.9999
		ARE(%)	**0.70**	**0.71**	**0.75**	**0.73**
AC-750	Langmuir	q_m (mmol g^{-1})	9.81	9.21	8.24	7.15
		K_L	0.0092	0.0071	0.0061	0.0055
		R^2	0.9945	0.9977	**0.9982**	0.9982
		ARE (%)	**4.10**	**3.80**	**2.94**	**2.53**
	Sips	q_{mS} (mmol g^{-1})	18.06	16.54	13.68	11.89
		$b(kPa)^{-n_S}$	0.0030	0.0024	0.0025	0.0023
		n_S	0.854	0.835	0.877	0.895
		R^2	0.9999	0.9998	0.9998	0.9998
		ARE(%)	**0.70**	**0.77**	**0.70**	**0.67**
AC-800	Langmuir	q_m (mmol g^{-1})	10.92	10.01	9.50	8.35
		K_L	0.0091	0.0079	0.0061	0.0054
		R^2	0.9972	0.9983	0.9986	0.9991
		ARE (%)	**5.23**	**3.83**	**3.68**	**2.96**
	Sips	q_{mS} (mmol g^{-1})	14.69	15.29	13.45	12.09

		$b(kPa)^{-n_S}$	0.0048	0.0034	0.0031	0.0027
		n_S	0.831	0.836	0.864	0.887
		R^2	0.9999	0.9999	0.9999	0.9999
		ARE(%)	**0.65**	**0.62**	**0.63**	**0.71**
AC-850	Langmuir	q_m (mmol g^{-1})	10.42	9.61	8.30	7.25
		K_L	0.0085	0.0069	0.0060	0.0053
		R^2	0.9944	0.9954	0.9947	0.9949
		ARE(%)	**3.93**	**3.17**	**2.70**	**2.39**
	Sips	q_{mS} (mmol g^{-1})	18.16	19.44	16.08	13.96
		$b(kPa)^{-n_S}$	0.0031	0.0021	0.0021	0.0020
		n_S	0.870	0.865	0.900	0.913
		R^2	0.9997	0.9999	0.9999	0.9999
		ARE(%)	**0.73**	**0.60**	0.52	0.51

**** Isosteric heat of adsorption***

To characterize and optimize the adsorption process, isosteric heat of adsorption (Q_{st}) is one of the requirement factors. The Q_{st} is a differential heat, defined as the heat of adsorption at a constant amount of adsorbate adsorbed. The Q_{st} can be obtained by assessing adsorption isotherms at different temperatures using the Clausius - Clapeyron equation [14]

$$\frac{d\ln P}{dT} = \frac{Q_{st}}{RT^2} \tag{4}$$

The integration form can be written as

$$\ln P = -\frac{Q_{st}}{R}\frac{1}{T} + \text{const} \tag{5}$$

The equilibrium pressure (P) at a constant amount of CO_2 adsorbed is obtained from the isotherm data at different temperatures. According to the best-fit model, the calculated parameter of the Sips equation (Table 5) was used to calculate the P value at constant q_e of 0.1, 0.5, 1.0, 1.5, and 2.0 mmol g^{-1} with the following equation:

$$\ln P = \frac{1}{n_S}\ln\left(\frac{q_e}{q_{ms} - q_e}\right) - \ln b \tag{6}$$

Figure 5 presents the plots of the logarithm of the equilibrium pressure (lnP) against the reciprocal temperature (1/T) at different q_e of AC samples. Isosteric heats of adsorption were calculated using the slopes obtained from Figure 5 and were summarized in Table 5, the R^2 values were also listed.

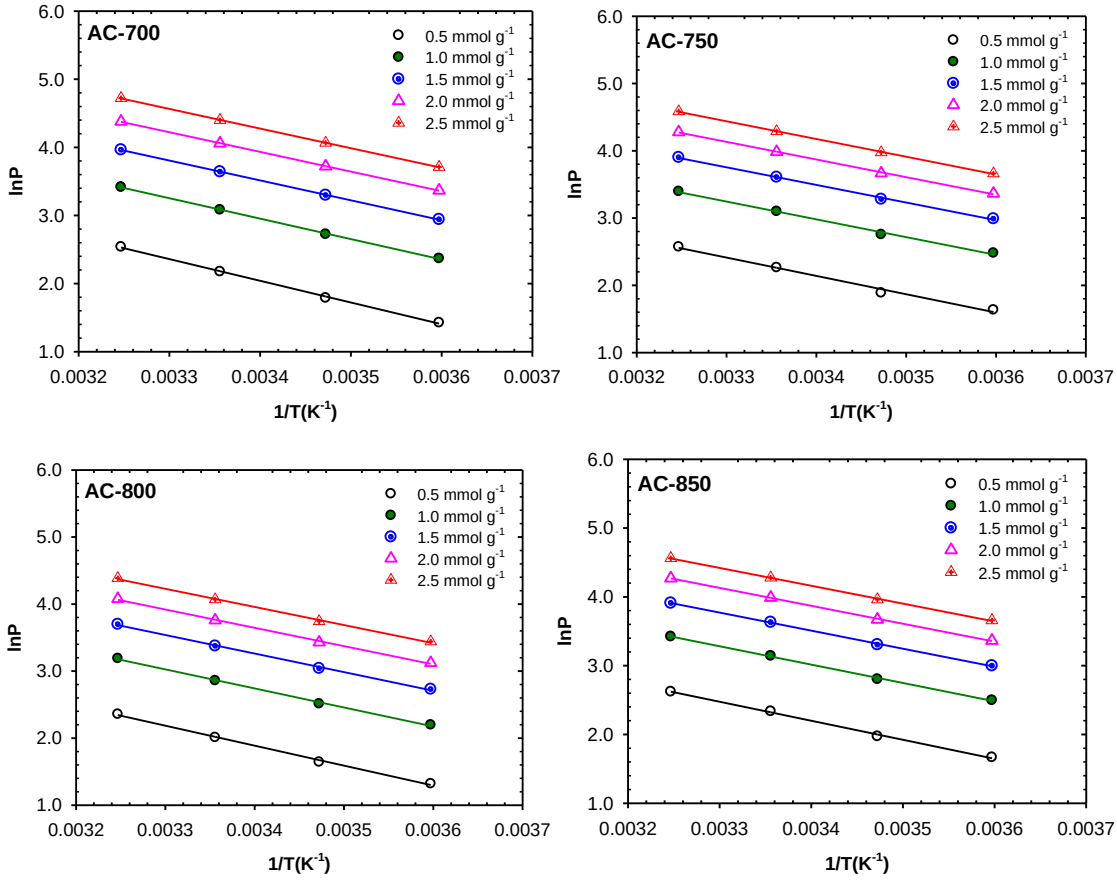

Figure 5. Plots of lnP against 1/T for CO_2 adsorption onto corn cob-activated carbon

Table 5. Isosteric heat of CO_2 adsorption on corn cob activated carbon

q_e (mmol g^{-1})	**AC-700**		**AC-750**		**AC-800**		**AC-850**	
	Q_{st} (kJ mol^{-1})	R^2	Q_{st} (kJ mol^{-1})	R^2	Q_{st} (kJ mol^{-1})	R^2	Q_{st} (kJ mol^{-1})	R^2
0.5	26.48	0.9988	22.65	0.9917	24.73	0.9975	22.97	0.9978
1.0	24.94	0.9987	21.97	0.9965	23.60	0.9982	22.16	0.9990
1.5	24.27	0.9999	21.76	0.9984	23.03	0.9983	21.79	0.9994
2.0	24.01	0.9999	21.78	0.9992	22.69	0.9983	21.62	0.9995
2.5	23.99	0.9999	21.94	0.9996	22.51	0.9981	21.55	0.9995

At the surface coverage between 0.5 and 2.5 mmol g^{-1}:

(i) Q_{st} for the adsorption of CO_2 of all activated carbon were in the range of 21.55 and 26.48 kJ mol^{-1}, which was the range for physical adsorption that allows for easy regeneration of the materials. These Q_{st} values are comparable with those reported for CO_2 adsorption onto carbon materials [17]. The sign of the isosteric heat is always the opposite sign of adsorption heat, thus adsorption heat is negative, suggesting an exothermic adsorption, which is in accordance with the result mentioned above.

(ii) For all samples Q_{st} decreased with the increase in the CO_2 surface coverage, which is the behavior of heterogeneity in the adsorption sites. Q_{st} was influenced by both the CO_2-AC (exothermic effect) and CO_2-CO_2 (endothermic effect) interactions [18], [19]. At high CO_2 loading, CO_2-AC interaction decreased universally, since the most active adsorption sites were filled, leaving less favorable binding sites. However, as the density of the gas increases, lessening the distance between CO_2 molecules, the CO_2-CO_2 interaction is more favorable, which in turn causes a decrease in Q_{st}.

(iii) Q_{st} of AC-700, AC-750, AC-800, and AC-850 samples oscillate between 26.48 - 23.99, 22.65 - 21.94, 24.73 - 22.51, and 22.97 - 21.55 kJ mol^{-1}, respectively. At the same surface loading, Q_{st} decreases in the order: AC-700 > AC-800 > AC-750 > AC-850. As indicated above, the carboxyl group present on the surface of AC can interact with CO_2, increasing the CO_2 adsorption capacity of the samples. The interaction between the carboxyl group and CO_2 releases energy, and the number of carboxyl groups of AC-700 (1.365 mmol g^{-1}) > AC-800 (0.769 mmol g^{-1}) > AC-750 (0.557 mmol g^{-1}) > AC-850 (0.450 mmol g^{-1}). This contributes to the interpretation of the decrease of Q_{st}.

3. Conclusions

Corn cob-activated carbons obtained using chemical activation with KOH were used for CO_2 adsorption at 5, 15, 25, and 35ºC. The correlation between the four fitting models was Sips > Tóth > Freudlich > Langmuir. A high adsorption capacity of CO_2 with the maximum monolayer coverage capacity was in the range of 6.28 - 10.92 mmol g^{-1}, which was deduced from the Langmuir equation. Isosteric heat of adsorption was in the range of 26.48 - 21.55 kJ mol^{-1} at five surface loadings from 0.5 to 2.5 mmol g^{-1} with an interval of 0.5 mmol g^{-1}. The adsorption capacity and the isosteric heat of adsorption of the AC samples depended on both the specific surface area and the amount of carboxylic groups. A high specific surface area and a high amount of carboxylic groups increased the adsorption capacity and isosteric heat of the adsorption of CO_2. This result showed the potential for the valorization of corn cob waste by the prepared activated carbon toward the application of CO_2 adsorption.

REFERENCES

[1] Lee ZH, Sethupathi S, Lee KT, Bhatia S, Mohamed AR, (2013). An overview on global warming in Southeast Asia: CO_2 emission status, efforts done, and barriers. *Renewable and Sustainable Energy Reviews*, 28, 71-81.

[2] International Council on Clean Transportation, EU CO_2 emission standards for passenger cars and light-commercial vehicles, Retrieved 5 February 2014.

[3] Leung DYC, Caramanna G, Maroto-Valer MM, (2014). An overview of the current status of carbon dioxide capture and storage technologies. *Renewable and Sustainable Energy Review*, 39, 426-443.

[4] Mofarahi M, Gholipour F, (2014). Gas adsorption separation of CO_2/CH_4 system using zeolite 5A. *Microporous and Mesoporous Materials*, 200, 1-10.

[5] Wickramaratne NP, Xu J, Wang M, Zhu L, Dai L, Jaroniec M, (2014). Nitrogen enriched porous carbon spheres: Attractive materials for supercapacitor electrodes and CO_2 adsorption. *Chemistry of Materials*, 26(9), 2820-2828.

[6] Loganathan S, Tikmani M, Edubilli S, Mishra A, Ghoshal AK, (2014). CO_2 adsorption kinetics on mesoporous silica under a wide range of pressure and temperature. *Chemical Engineering Journal*, 256, 1-8.

[7] Liu J, Thallapally PK, McGrail BP, Brown DR, Liu J, (2012). Progress in adsorption-based CO_2 capture by metal-organic frameworks. *Chemical Society Reviews*. 41, 2308-2322.

[8] Pedroza MM, Machado PRS, Silva JGD, Arruda MG, Picanco AP, (2023). Production and application of activated carbon obtained from the thermochemical degradation of corn cob. *Journal of Applied Research and Technology*, 21, 952-964.

[9] Le VK, Dang VC, Luong TTT, (2016). Investigation of the Capacitive Properties of Activated Carbon Prepared from Corn Cob in Na_2SO_4 and K_2SO_4 Electrolytes. *Canadian Chemical Transactions*, 4(3) 302-315.

[10] N. Rambabu, R. Azargohar, A.K. Dalai, J. Adjaye, (2013). Evaluation and comparison of enrichment efficiency of physical/chemical activations and functionalized activated carbons derived from fluid petroleum coke for environmental applications. *Fuel Process Technology*, 106, 501-510.

[11] Figueiredo JL, Pereira MFR, Freitas MMA, Orfao JJM, (1999). Modification of the surface chemistry of activated carbon. *Carbon*, 37, 1379-1389.

[12] Petrovic B, Gorbounov M, Soltani SM, (2022), Impact of surface functional groups and their introduction methods on the mechanisms of CO_2 adsorption on porous carbonaceous adsorbents. *Carbon Capture Science and Technology*, 3, article ID: 100045.

[13] Khosrowshahi MS, Abdol MA, Mashhadimoslem J, Khakpour E, Emrooz HBM, Sadeghzadeh S, Ghaemi A, (2022). The role of surface chemistry on CO_2 adsorption in biomass-derived porous carbons by experimental results and molecular dynamics simulations, *Science Reports*, 12, Article ID: 8917.

[14] Siperstein FR, Avendano C, Ortiz JJ, Gil-Villegas A, (2021). Analytic expressions for the isosteric heat of adsorption from adsorption isotherm models and two-dimensional SAFT-VR equation of state. *AIChE Journal*, 67, article ID: e17186.

[15] Akpasi SO, Isa YM, (2022). Effect of operating variables on CO_2 adsorption capacity of activated carbon, kaolinite, and activated carbon – kaolinite composite adsorbent. *Water-Energy Nexus*, 5, 21-28.

[16] Fatima SS, Borhan A, Ayoub M, Ghani NA, (2023). Modeling of CO_2 adsorption on Surface-Functionalized Rubber-Seed Shell Activated Carbon: Isotherm and Kinetic Analysis. *Processes*, 11(10, article ID: 2833.

[17] Choma J, Stachurska K, Marsweuski, M, Jaroniec M, (2016). Equilibrium isotherms and isosteric heat for CO_2 adsorption on nanoporous carbons from polymers. *Adsorption*, 22, 581-588.

[18] Ma X, Li Y, Cao M, Hu Changwen, (2014). A novel activating strategy to achieve highly porous carbon monoliths for CO_2 capture, *Journal of Materials Chemistry A*, 2, 4819-4826.

[19] Simmons JM, Wu H, Zhou W, Yildrim T, (2011). Carbon capture in metal-organic frameworks – a comparative study. *Energy and Environmental Science*, 4, 2177-2185.